Radiation Physics and Chemistry 78 (2009) 1102–1105

Contents lists available at ScienceDirect

Radiation Physics and Chemistry

journal homepage: www.elsevier.com/locate/radphyschem

Measurement of coherent terahertz radiation for time-domain spectroscopy and imaging

R. Kuroda *, M. Yasumoto, N. Sei, H. Toyokawa, H. Ikeura-Sekiguchi, H. Ogawa, M. Koike, K. Yamada

Research Institute of Instrumentation Frontier, National Institute of Advanced Industrial Science and Technology (AIST), Central 2, 1-1-1 Umezono, Tsukuba, Ibaraki 305-8568, Japan

ARTICLE INFO

Keywords:
Terahertz
Time-domain spectroscopy
THz-TDS
THz imaging
Linac
Electron beam
Laser

ABSTRACT

A high-power terahertz (THz) source for THz time-domain spectroscopy (THz-TDS) and THz imaging has been developed based on an S-band compact electron linac at the National Institute of Advanced Industrial Science and Technology (AIST). A THz pulse was generated as coherent synchrotron radiation (CSR) from an ultra-short electron bunch and expected to have peak power of kW-order with frequency range of 0.1–2 THz. The electro-optic (EO) sampling method with a ZnTe crystal for the THz pulse measurement has been prepared for THz-TDS system. The timing measurement between the THz pulse and a probe laser was carried out. A preliminary experiment of THz transmission imaging of an integrated circuit (IC) card has been successfully demonstrated using the THz CSR pulse and a W-band rf detector. The imaging result was experimentally compared with a result of X-ray imaging. It is confirmed that its intensity and stability are enough to perform for the THz applications.

1. Introduction

Terahertz (THz) radiation is an electromagnetic radiation in the range between millimeter waves and far infrared. It is a useful tool for progressing on biomedical and material studies such as THz imaging (Mittleman et al., 1996) and THz time-domain spectroscopy (THz-TDS) (Exter et al., 1989). The THz-TDS has recently emerged as a powerful probe of charge transport in materials, owing to the fact that it provides a probe of the complex conductivity in a wide frequency range with sub-picosecond time resolution (Kawayama et al., 2002). The THz imaging technology is expected to generate many novel applications such as non-destructive inspection in commercial industries and security systems, and medical diagnosis (Kawase et al., 2003). However, the investigation of the sample which has large absorption in the THz region is not practical using a conventional THz source based on a femtosecond mode-locked laser due to its lack of power. Especially, it is difficult to investigate liquid materials including bio-specimens because water is opaque to THz. A high peak power THz source is required instead of the conventional source whose typical peak power is about 10 mW. Consequently, the high-power THz source is also necessary for THz-TDS and imaging system.

On the other hand, a high-power THz source based on coherent synchrotron radiation (CSR) whose peak power is kW-order has been established in the previous report using an S-band compact electron linac at the National Institute of Advanced Industrial Science and Technology (AIST) in Japan (Kuroda et al., 2008a). The CSR THz pulse can be generated in a wavelength between 150 μm–3 mm (0.1–2 THz) using an ultra-short electron bunch. We have started to apply the high-power THz source to the THz-TDS system (Kuroda et al., 2008b) and the THz imaging system.

2. High-power THz source

Fig. 1 shows a top view of the THz-TDS system and the imaging system based on the S-band compact electron linac. Total system was installed in a middle size room of about $10 \times 10\,m^2$ including all components. The S-band linac has an electron injector, an achromatic arc section for a bunch compressor, a 90° bending magnet and laser systems. The electron injector consists of a laser photocathode rf gun which has the BNL-type S-band 1.6 cell cavity with a Cs_2Te photocathode load-lock system and a solenoid magnet for the emittance compensation. The low-emittance electron beam with more than 1 nC can be generated and accelerated up to about 40 MeV using the S-band linac and the rf source of a 20 MW klystron. The electron bunch was compressed to less than 1 ps with the magnetic bunch compressor. The coherent synchrotron radiation of the THz region was generated from the ultra-short and high-charge electron bunch at the 90° bending magnet located at the end of the beam line downstream from the bunch compressor (Kuroda. et al., 2008a). The THz CSR pulse is extracted from a z-cut quartz window for THz applications. Typical electron beam parameters for the THz CSR generation and our expected THz specification

* Corresponding author. Tel.: +81 29 861 5104; fax: +81 29 861 5683.
E-mail address: ryu-kuroda@aist.go.jp (R. Kuroda).

0969-806X/$ - see front matter
doi:10.1016/j.radphyschem.2009.06.026

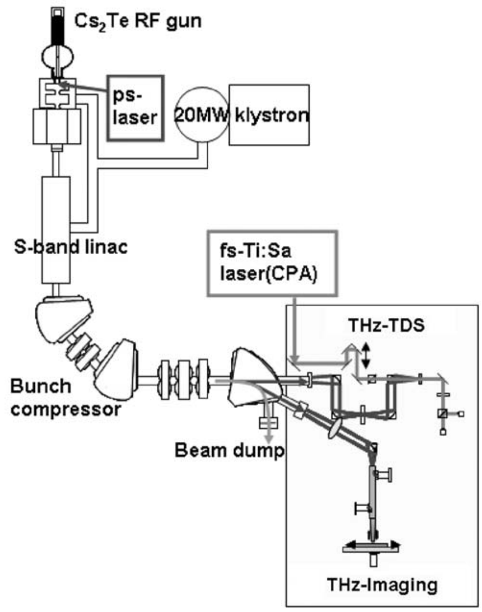

Fig. 1. THz-TDS system and imaging system based on S-band compact electron linac.

Table 1
Parameters of electron beam and expected THz specification.

Electron beam	
Max. energy	30–42 MeV
Charge per bunch	1–2 nC
Energy spread for compression	~5%
Bunch length (after compression)	300 fs (rms)
Bunch number	1–100
Rep. rate	10–50 Hz
THz pulse	
Frequency	0.1–2 THz
Pulse energy	65 nJ
Peak power	25 kW
Rep. rate	10–50 Hz
Pulse width	700 fs (rms)

were described in Table 1. The observed temporal width of the CSR pulse depends on the frequency response of the measurement system. In this system with the electro-optic (EO) sampling method, it is supposed to be about 700 fs (rms) because of the frequency response of the quartz window, the EO crystal and the detector.

3. Development for THz applications

3.1. Preparation of THz-TDS system with the EO sampling method

The THz-TDS system based on the S-band electron linac has been designed in our previous report (Kuroda et al., 2008b). The THz CSR pulse is generated from the ultra-short electron bunch and extracted from the z-cut quartz window and focused to a sample using off-axis parabolic mirrors. Transmitted THz pulse is detected by the electro-optic sampling method (Chen et al., 2001) using a EO crystal such as a ZnTe and a femtosecond Ti:Sa laser as a probe laser. The probe pulse passes through an optical delay stage and a polarizer for high linear polarization. The linearly polarized probe pulse and the THz pulse are co-propagated

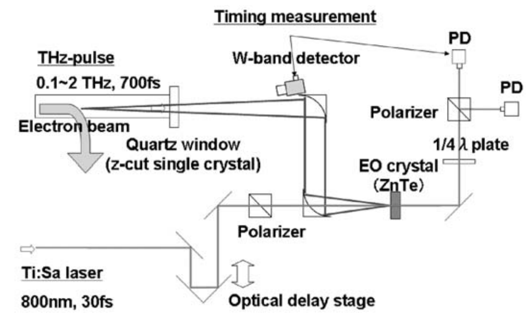

Fig. 2. Setup for temporal profile measurement of THz pulse and timing measurement between THz pulse and probe laser pulse.

Fig. 3. Holder-mounted ZnTe [1 1 0] crystal as high resistivity EO crystal.

through the [1 1 0]-oriented ZnTe crystal. The transmitted probe pulse passes through a quarter wave plate and an analyzing polarizer. The phase retardation of the probe laser is obtained by measuring the deference between two signals with two photo-diodes (PDs). The phase retardation of the probe laser is in proportion to the intensity of THz electric fields. The THz pulse temporal waveform can be measured by the pump-probe method with the optical delay stage. The spectra and phase information of the THz pulse are obtained by the Fourier transform of the measured waveform. The absorption characteristics of a sample in the THz region are obtained from the deference of the spectrum due to no-insertion and insertion of the sample.

As a first step for the THz-TDS system, the temporal profile measurement of THz pulse was designed in Fig. 2. The EO crystal shown in Fig. 3 was selected as a [1 1 0]-oriented ZnTe crystal (Ingcrys Laser Systems Ltd.) which has high resistivity about 10^3–$10^4\,\Omega$/cm with $10 \times 10 \times 0.5\,mm^3$ in size. The preliminary experiment of the timing measurement between the THz pulse and the probe laser has been demonstrated using the W-band rf detector and the photo-diode detector, respectively. These signals are combined by the signal combiner in order to deliver with one cable for a long distance to the measurement room outside of the accelerator room. In Fig. 4, the time difference is preliminarily measured and expected to be about 6 ns in correspondence to the optical path length of about 1.8 m. In the next step, the optimum timing survey will be done using the optical delay stage and the